



Thank you for downloading this document from the RMIT Research Repository.

The RMIT Research Repository is an open access database showcasing the research outputs of RMIT University researchers.

RMIT Research Repository: <http://researchbank.rmit.edu.au/>

Citation:

Zhang, X, Fan, L and Roddick, F 2014, 'Feedwater coagulation to mitigate the fouling of a ceramic MF membrane caused by soluble algal organic matter', *Separation and Purification Technology*, vol. 133, pp. 221-226.

See this record in the RMIT Research Repository at:

<https://researchbank.rmit.edu.au/view/rmit:24750>

Version: Accepted Manuscript

Copyright Statement: © 2014 Elsevier B.V. All rights reserved.

Link to Published Version:

<http://dx.doi.org/10.1016/j.seppur.2014.06.053>

PLEASE DO NOT REMOVE THIS PAGE

28 **1 Introduction**

29 Ceramic microfiltration (MF) and ultrafiltration (UF) membranes are increasingly
30 utilised in water and wastewater treatment due to their inherent advantages such as high
31 mechanical stability, chemical stability and high hydrophilicity over conventional low-
32 pressure polymeric membranes [1, 2]. However, membrane fouling due to the attachment of
33 aquatic organic matter on the surface and/or inner structures of the membranes remains a
34 major issue limiting the efficiency of ceramic membrane water treatment systems [3].

35

36 Blooms of cyanobacteria (also referred to as blue-green algae) occur frequently in
37 many drinking water catchments and result in the release of a substantial amount of soluble
38 algal organic matter (AOM) to the downstream water treatment systems, causing great
39 concerns about water quality and treatment efficiency [4]. The predicted increase in average
40 temperature due to climate change is likely to lead to a higher frequency of cyanobacterial
41 blooms in the future [5]. The AOM released from the cyanobacteria is usually hydrophilic in
42 nature and comprises mainly proteins and polysaccharides [6] which have been
43 demonstrated to have high fouling potentials for both polymeric and ceramic water treatment
44 membranes. The membrane fouling caused by AOM led to severe permeate flux decline in
45 constant transmembrane pressure filtration or significant pressure increase in constant flux
46 mode [6-9]. A recent study on the AOM fouling of a commercial ceramic MF membrane
47 revealed that the majority of the flux decline was attributed to the very high molecular weight
48 (MW) biopolymer compounds, which resulted in the formation of an outer fouling layer of
49 high filtration resistance [7].

50

51 Feedwater pre-treatment is a common approach to transform/remove the high fouling
52 potential components, and consequently mitigate their propensity to foul the water treatment
53 membranes [8]. Among the various pre-treatment methods, chemical coagulation with
54 aluminium based salts or ferric based salts is widely used for the removal of high molecular

55 weight organics from water and waste water [9, 10]. The effectiveness of organic removal
56 through coagulation can be strongly affected by the characteristics of the feedwater, and the
57 type and dose of the coagulant [11]. A previous study showed alum and ACH could improve
58 the filterability of a biologically treated municipal wastewater containing the AOM derived
59 from *Microcystis aeruginosa* for a polymeric MF membrane [12]. However, comparison of the
60 effect of the most commonly used water treatment coagulants (such as aluminium and iron
61 based coagulants) in reducing AOM fouling for ceramic membranes has not been
62 documented.

63

64 The aim of the present study is to evaluate the fouling mitigation effect of four widely
65 used water treatment coagulants, i.e., alum, ACH, $\text{Fe}_2(\text{SO}_4)_3$ and FeCl_3 , on the water
66 containing AOM using a lab scale ceramic MF membrane system. The AOM used in the
67 work was extracted from stationary growth phase cultures of *Microcystis aeruginosa* which is
68 the most prevalent cyanobacterium worldwide [13]. The effect of the coagulation on
69 membrane fouling was characterised in terms of reduction in reversible and irreversible
70 fouling resistance, dissolved organic carbon, carbohydrate and protein contents. Advanced
71 organic characterisation techniques including size exclusion chromatography (SEC) using
72 liquid chromatography with organic carbon detection (LC-OCD), fluorescence excitation-
73 emission matrix (EEM) spectra and fractionation using resin adsorption chromatography
74 were also employed, with a view to obtaining better insights into the effect of coagulation on
75 fouling mitigation.

76

77 **2 Experimental**

78 2.1. Cultivation of cyanobacteria, AOM extraction and preparation of feed solutions

79 *M. aeruginosa* (CS 566/01-A01) was purchased from the CSIRO Microalgae
80 Research Centre (Tasmania, Australia). The algal cultures were grown in 5 L Schott bottles
81 using MLA medium [14] under humidified aeration. The cultures were placed in an incubator

82 at the temperature of 22 °C under illumination for 12 h/day. The AOM was extracted from
83 cultures harvested after 35th day of growth (stationary growth phase) by centrifugation (3270
84 × g for 30 mins) of the cell suspensions, and the subsequent filtration of the supernatant
85 using 1 µm membranes (Whatman® Grade GF/A). To mimic the presence of AOM in
86 drinking water, the extracted AOM was diluted to a DOC concentration of 4.3 ± 0.2 mg/L with
87 tap water (1.4 ± 0.05 mg DOC/L) to make the feedwater for the coagulation or MF tests. The
88 pH of the AOM solution was adjusted to 8.0 ± 0.2 using 1 M HCl or 1 M NaOH prior to the
89 coagulation tests.

90

91 2.2. Microfiltration tests

92 A 7-channel tubular ceramic ZrO₂-TiO₂ MF membrane with a nominal pore size of 0.1
93 µm (CeRAM™ INSIDE, TAMI Industries) was used in the filtration experiments and operated
94 under dead-end mode. The ceramic membrane surface layer was made of ZrO₂ and the
95 support layer was made of TiO₂. This membrane surface was considered as hydrophilic
96 (ZrO₂ based membrane usually has a contact angle less than 20°) due to the presence of
97 surface hydroxyl groups [15]. All filtration runs were carried out at a constant transmembrane
98 pressure (TMP) of 70 ± 1 kPa at room temperature (22 ± 2 °C) for 90 min. After each MF test,
99 the membrane was backwashed for 2 minutes with tap water. The same membrane was
100 used for all MF runs, and after each run the membrane was restored by Cleaning in Place
101 (CIP) by using 0.05 M NaOH and 0.05 M HNO₃ solution until the permeate flux reached 170-
102 180 LMH.

103

104 The reversible and irreversible fouling resistance were determined with the following
105 equations:

$$106 \quad J = \frac{\Delta P}{\mu R_{total}} \quad (1)$$

$$107 \quad R_{total} = R_{reversible} + R_{irreversible} + R_{membrane} \quad (2)$$

108 Where ΔP is the transmembrane pressure; J stands for the permeate flux and μ is the water
109 viscosity at 22 °C (0.955×10^{-3} Pa s). R_{total} refers to the total resistance after MF of an AOM
110 solution, which can be calculated using the permeate flux at the end of the filtration. $R_{reversible}$
111 is associated with the hydraulically reversible fouling resistance, and can be determined
112 using the flux before and after backwash with tap water. $R_{membrane}$ is the resistance of a clean
113 membrane, which was determined by the tap water flux prior to the filtration test with an
114 AOM solution. $R_{irreversible}$ is the hydraulically irreversible fouling resistance, and can be
115 calculated by deducting $R_{reversible}$ and $R_{membrane}$ from R_{total} .

116

117 2.3. Coagulation conditions

118 Coagulation using ACH (aluminium chlorohydrate, Megapac 23, 40% w/w), alum,
119 ferric chloride and ferric sulphate were investigated as the pre-treatment for AOM solution.
120 Coagulation was conducted at room temperature ($20 \pm 2^\circ\text{C}$) in a laboratory jar tester unit
121 (Phipps and Bird, PB-700) with rapid mixing for 1 min at 200 rpm, followed by slow mixing for
122 20 min at 30 rpm. A range of dosages (1-20 mg Al^{3+}/L or 1-20 mg Fe^{3+}/L) was tested to
123 determine the optimal dosage for organic removal. After the jar tests, the resultant treated
124 water samples were immediately filtered with 5 μm filter (Advantec) to remove the flocs in
125 the coagulated solution and the pH of the filtrate was adjusted to 8 prior to being fed to the
126 ceramic membrane MF rig.

127

128 2.4. Analytical methods

129 DOC and UV absorbance at 254 nm (UVA_{254}) were determined using a Sievers 820
130 TOC analyser and a UV/Vis spectrophotometer (UV2, Unicam), respectively. pH was
131 measured with a Hach Sension 156 pH meter. The phenol-sulphuric method was used to
132 determine carbohydrate content [16] with D-glucose used as the standard carbohydrate
133 substance. Protein content was measured using the bicinchoninic acid (BCA) method for
134 which the QPBCA QuantiPro™ BCA Assay Kit (Sigma Aldrich) was utilised. Bovine serum
135 albumin (Sigma Aldrich) was used as the standard protein substance.

136

137 Fluorescence excitation-emission matrix (EEM) spectra were obtained using a fluorescence
138 spectrometer (LS 55, PerkinElmer) at an excitation and emission wavelength range of 200–
139 550 nm. An interpolation method [17] was used to remove the first-order Rayleigh scattering.
140 The second-order Rayleigh scattering was limited by using a 290 nm emission cut off filter.
141 The fluorescence spectra of deionised water were subtracted from all EEM spectra to
142 remove the Raman scattering and other background noise.

143

144 The apparent molecular weight distribution of the AOM was determined by SEC with LC-
145 OCD at the Water Research Centre of the University of New South Wales, Sydney,
146 Australia. The LC-OCD system (LC-OCD Model 8, DOC-Labor Dr. Huber, Germany) utilised
147 a SEC column (Toyopearl TSK HW-50S, diameter 2 cm, length 25 cm) and the
148 chromatograms were processed using the Labview based program Fiffikus (DOC-Labor Dr.
149 Huber, Germany). The details of this technique are described by Huber et al. [18].

150

151 Nonionic macro-porous resins (DAX-8 and XAD-4) were employed to separate the organics
152 into hydrophobic (HPO), transphilic (TPI) and hydrophilic (HPI) fractions. More details of the
153 organic matter fractionation procedure can be found elsewhere [19]. All filtration tests were
154 duplicated and analyses triplicated, and reported in terms of mean value and error/standard
155 deviation.

156

157 2.5. Membrane fouling analysis using classic filtration models

158 Hermia's constant pressure filtration models including complete blocking, standard blocking,
159 intermediate blocking and cake filtration have been widely used to interpret the filtration
160 behaviour of dead-end membrane filtration systems [20]. The detailed description of these
161 models can be found from Shen et al. [21]. The equations for these models are shown in
162 Table 1. The identification of the key fouling mechanism in this study was conducted

163 by fitting the experimental data to the equations (Eqs. 3-6). The resulting R -squared
164 (R^2) value was used to indicate the goodness of the fit.

165

166 **Table1.** Equations for classic filtration models [22].

Law	Equation
Complete blocking	$J_0 - J = aV$ (3)
Intermediate blocking	$1/J - 1/J_0 = bt$ (4)
Standard blocking	$t/V = ct + d$ (5)
Cake filtration	$1/J - 1/J_0 = eV$ (6)

167

168 Where V is the cumulative volume of permeate at time t , J and J_0 represent flux and initial
169 flux respectively. a , b , c , d , e are the model parameters, which could be obtained from data
170 fitting.

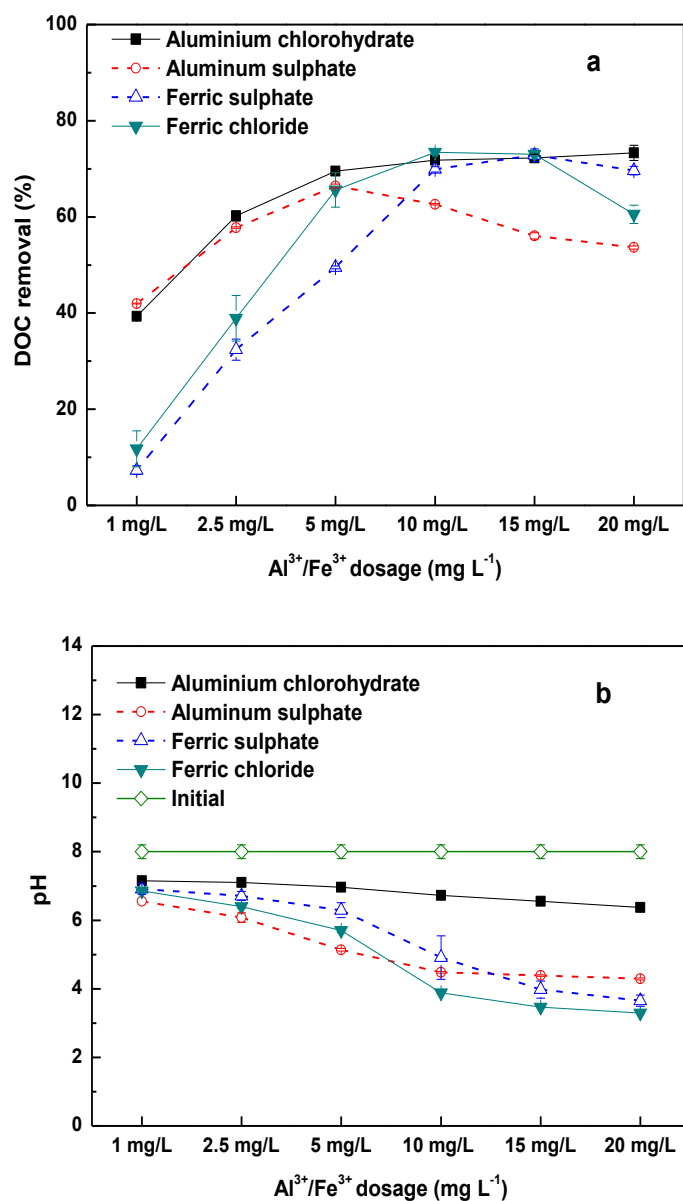
171

172 **3. Results and discussion**

173 **3.1 Optimum coagulant dosages**

174 For the two aluminium based coagulants, the organic matter removal increased
175 significantly with increasing the Al^{3+} dosage from 1 to 5 mg/L, with 70% and 65% of DOC
176 reduction for ACH and alum at 5 mg Al^{3+} /L, respectively (Fig. 1a). On increase of the
177 dosages from 10 to 20 mg Al^{3+} /L, there was no further increase in DOC reduction for ACH
178 but a considerable decrease for alum. For the iron based coagulants, the DOC removal
179 increased with increasing iron dosage and was maximum at about 10 mg Fe^{3+} /L, with
180 approximately 70% of DOC was removed by the coagulation with the two coagulants. The
181 optimum coagulant dosages in terms of DOC reduction for the AOM solutions were therefore
182 determined as 5 mg Al^{3+} /L for ACH and alum, and 10 mg Fe^{3+} /L for $Fe_2(SO_4)_3$ and $FeCl_3$.
183 Coagulation with ACH did not significantly alter the pH of the AOM solutions, and the pH of

184 the coagulated water was maintained at around 7 for all dosages (Fig. 1b). Coagulation with
 185 alum, $\text{Fe}_2(\text{SO}_4)_3$ and FeCl_3 at their optimum dosages greatly reduced the solution pH. As the
 186 solution pH could affect the MF performance, the pH of all coagulated solutions was
 187 adjusted to 8 prior to all filtration tests for the purpose of a better comparison.
 188



189

190

191 **Fig.1** Comparison of DOC removal and pH change for the four coagulants: a) DOC removal,

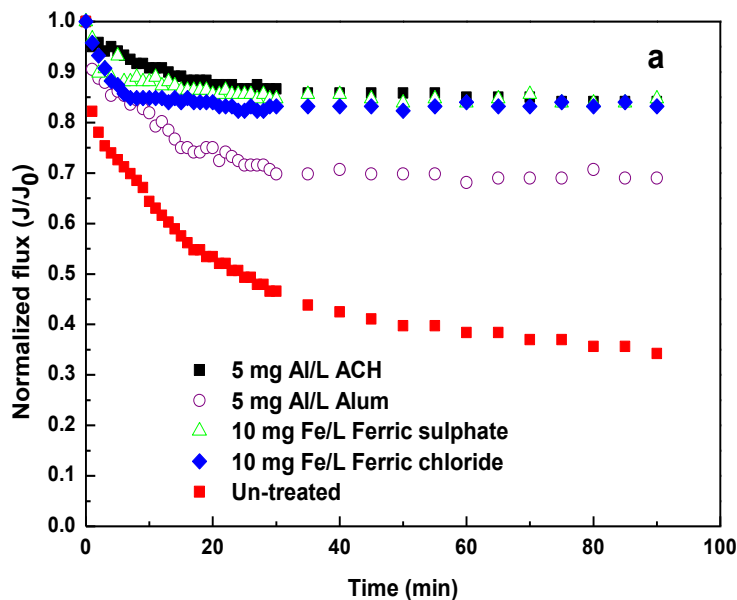
192

b) pH of the coagulated AOM solutions

193

194 3.2 Microfiltration tests

195 The AOM solution without pre-treatment caused rapid and severe flux decline, with
196 approximately 55% reduction in flux at the end of the filtration (Fig. 2a). Feedwater pre-
197 treatment by coagulation reduced the flux decline significantly for all coagulants tested,
198 indicating the foulant causing severe flux reduction was effectively removed through the
199 coagulation process. Coagulation with ACH at 5 mg Al³⁺/L resulted in a slightly higher flux
200 compared with ferric chloride and ferric sulphate at 10 mg Fe³⁺/L in the initial 20 min of
201 filtration. After that the extent of flux reduction for the three coagulants became comparable
202 and approximately 15% of flux decline was obtained at the end of the filtration. Coagulation
203 with alum at 5 mg AL³⁺/L gave less flux improvement compared with other coagulants, with
204 around 25% of flux decline at the end of the filtration. Fouling resistance results indicated
205 both reversible and irreversible resistance were reduced markedly due to the coagulation of
206 the feedwater (Fig. 2b). The reduction in hydraulically reversible fouling was comparable for
207 the four coagulants (91-95%), whereas ACH and Fe₂(SO₄)₃ performed considerably better
208 than alum and FeCl₃ in reducing the irreversible fouling.



209

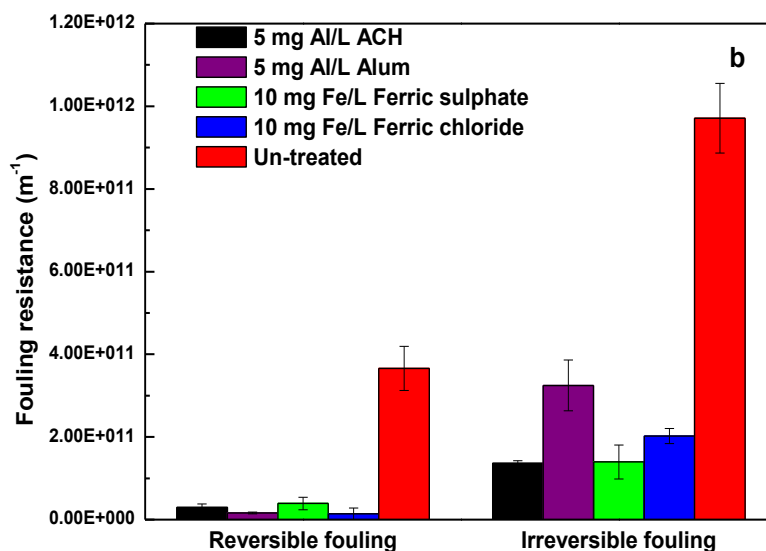
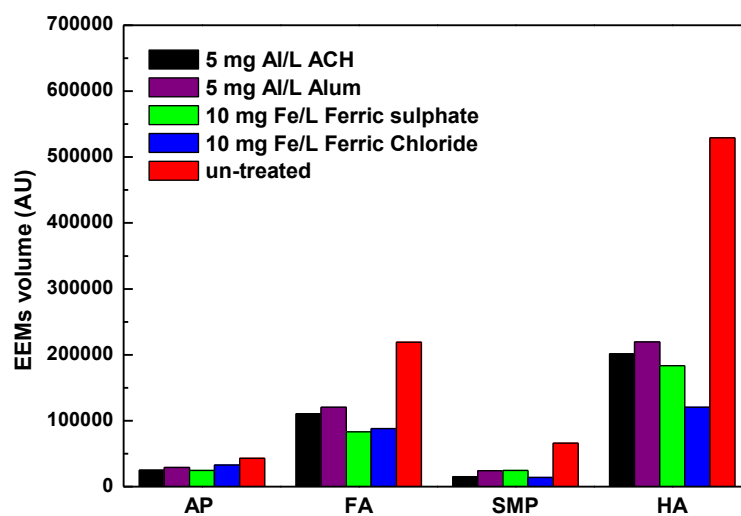


Fig.2 Comparison of (a) flux decline and; (b) fouling resistance in the MF of the un-coagulated and coagulated AOM solutions

3.3 Characterising the effect of coagulation by EEM spectra

Fluorescence EEM spectra have been employed as a useful tool in characterising aquatic organic matter including AOM [23]. EEM spectra can be divided into five regions. Regions I (Ex/Em: 220-270 nm/280-330 nm) and II (Ex/Em: 220-270 nm/330-380 nm) correspond to aromatic proteins (AP), and region III (Ex/Em: 220-270 nm/380-540 nm) is associated with fulvic acid (FA)-like substances. Regions IV (Ex/Em: 270-440 nm/280-380 nm) and V (Ex/Em: 270-440 nm/380-540 nm) represent soluble microbial products (SMPs, e.g., proteins and polysaccharide-like materials) and humic acid (HA)-like materials, respectively. The fluorescence regional integration (FRI) method was used to quantify the changes in the fluorescent organic species before and after the coagulation treatment [24]. All four coagulants gave greater reductions in HA-like (58-77%) and SMP (62-78%) substances than AP (25-41%) and FA-like (49-62%) substances (Fig. 3). Since the HA-like substances in AOM were shown to have less impact on the flux decline for the ceramic MF membrane compared with SMPs and AP [25], the results suggested the flux improvement in this study was primarily due to the removal of the SMPs. The removal in the SMPs by ACH

230 (77%) and FeCl₃ (78%) was greater than for alum (63%) and Fe₂(SO₄)₃ (62%), which was
 231 consistent with the resultant higher flux for the ACH and FeCl₃ treated water. Although
 232 relatively a lower SMP removal was observed for Fe₂(SO₄)₃ compared with ACH and FeCl₃,
 233 the Fe₂(SO₄)₃ treated water exhibited a similar permeate flux as the water treated by ACH
 234 and FeCl₃ (Fig. 2a). This was likely attributed to the better removal of AP (41%) and FA
 235 (62%) removal for Fe₂(SO₄)₃ than the other coagulants, since these organic substances also
 236 have high fouling potentials for the ceramic MF membrane [25].
 237



238
 239 **Fig.3** EEM spectra volumes for the AOM solutions before and after coagulation
 240

241 **3.4 Effect of coagulation on molecular weight of AOM**

242 The apparent molecular weight distribution of the AOM before and after coagulation
 243 treatment was examined using SEC with LC-OCD (Fig. 4). The untreated AOM solution
 244 contained significant amounts of very high molecular weight (MW) biopolymers (>> 20,000
 245 Da), including two peaks which appeared between 20 and 40 min retention time, medium-
 246 MW components (i.e., humic-like substances, ~1,000 Da and building blocks, 350-500 Da),
 247 and low-MW substances (< 350 Da). The organics associated with the second biopolymer
 248 peak (at around 38 min retention time) were likely mainly comprised of relatively lower MW

249 biopolymers such as small polysaccharides, polypeptides and polyamino acids in the AOM
250 solutions [5].

251

252 According to the LC-OCD data, over 90% of the very high MW biopolymers were
253 removed by the coagulation treatments. The iron based coagulants tended to remove more
254 humic-like compounds than the aluminum based coagulants (e.g., ~ 50% for $\text{Fe}_2(\text{SO}_4)_3$ and
255 FeCl_3 compared with 42% and 23% for alum and ACH). The results were consistent with
256 some published studies in which it was observed coagulation tended to remove more
257 macromolecules (such as biopolymers) than medium MW molecules (such as humic-like
258 substances) from the biologically treated municipal wastewater [9, 26]. The significant
259 reduction in flux decline after the coagulation treatment was therefore attributed to the
260 effective removal of the macromolecules, which helped to mitigate the formation of the high-
261 resistance outer fouling layer on the membrane [5].

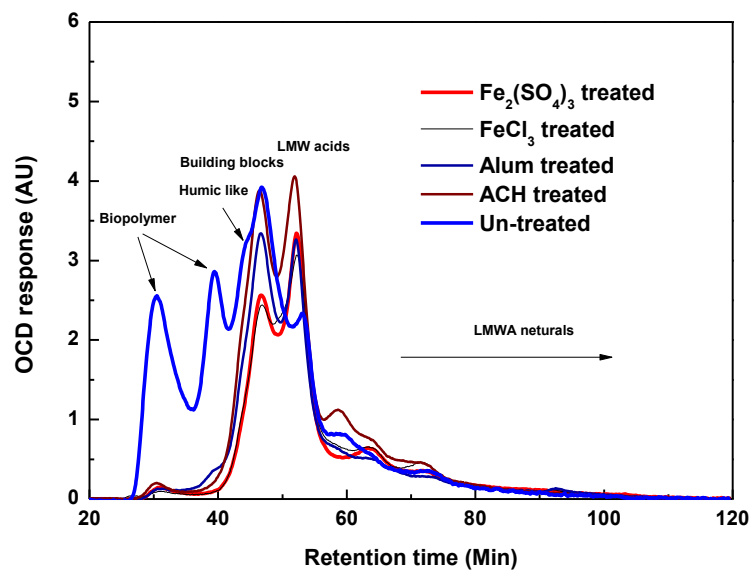
262

263 The greater removal of the high MW biopolymers during the coagulation was related
264 to the properties of these molecules. The high MW biopolymers mainly consist of
265 polysaccharides and proteinaceous materials [4]. The high MW polysaccharides (such as
266 transparent exopolymer particles) and proteins contained in AOM are reported to be very
267 surface active, as the metal-binding functional groups (such as carboxyl and hydroxyl groups)
268 in these organics are abundant [27]. Hence they could have strong potential to bind with
269 trivalent metals (such as Al^{3+} and Fe^{3+}) to form larger size complexes [28, 29]. However,
270 other coagulation mechanisms (such as sweep-floc and charge neutralization) may also
271 have contributed to the removal of the biopolymers during coagulation. This would be due to
272 the negatively charged AOM molecules (measured as -27 mV under the experimental
273 conditions), the coagulant dosage and solution pH (4-7) used, which are likely to lead to the
274 removal of the high MW molecules through these mechanisms [30].

275

276 It was observed that there was an increase in organic compounds with low MW
277 (<350 Da) after the coagulation, this was probably due to the breaking down of
278 macromolecules or the formation of some metal-organic complexes [31]. These compounds
279 were not likely to be retained by the ceramic MF membrane due to these molecules being
280 significantly smaller than the pore size of the membrane.

281



282

283 Fig.4. Comparison of LC-OCD chromatograms for the AOM before and after coagulation.

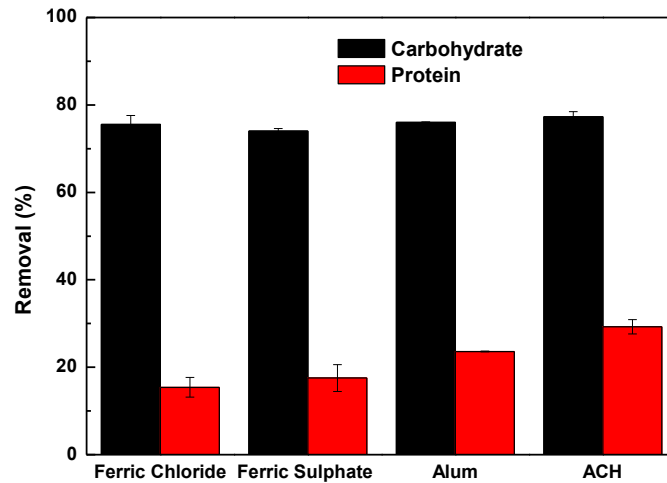
284

285 3.5 Effect of coagulation on carbohydrate and protein removal

286 As the biopolymers such as polysaccharides and proteins played an important role in
287 the membrane flux decline, the carbohydrate and protein content of the AOM before and
288 after the coagulation was analysed. The carbohydrate removal was similar for all types of
289 coagulant, with the removal efficiency of 74 - 77% (Fig. 5). However, the protein removal
290 efficiency for all types of coagulant was markedly lower (15-28%). The results suggested the
291 very high MW and high MW molecules removed by coagulation (as indicated in LC-OCD
292 chromatograms) were mainly consisted of carbohydrates (such as polysaccharides) instead
293 of proteins. Hence it appeared that the carbohydrate compounds in the AOM were more
294 susceptible to coagulation treatment. The relatively lower protein removal was probably

295 because some of the protein molecules had the capacity to form small complexes with
296 coagulants, which inhibit the coagulation efficiency [32].

297



298

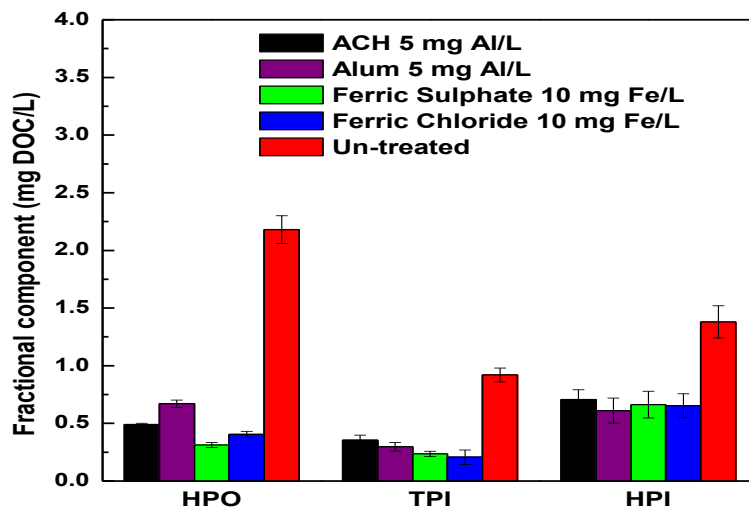
299 **Fig.5** Removal of carbohydrate and protein content from the untreated and coagulated AOM.
300 (The initial carbohydrate and protein concentration in un-treated solution was 5.2 ± 0.4 mg/L
301 and 2.0 ± 0.1 mg/L, respectively.)

302

303 3.6 Characterising the effect of coagulation by organic matter fractionation

304 The AOM before and after coagulation was fractionated into different organic groups
305 based on their hydrophobicity using resin adsorption chromatography. Our previous study
306 showed the HPO and HPI fractions of the AOM had significantly higher fouling potentials
307 than TPI in increasing flux decline and irreversible fouling resistance [25]. All coagulants
308 achieved significant reductions in all three fractions (Fig. 6). Coagulation tended to reduce
309 the HPO more than the TPI and HPI, with the average removal efficiencies of 78% for HPO,
310 70% for TPI and 52% for HPI. FeCl_3 and $\text{Fe}_2(\text{SO}_4)_3$ gave 85% and 81% reduction in HPO
311 compounds, which were considerably higher than ACH (77%) and alum (69%). It appeared
312 the iron based coagulants were more effective in removing the HPO compounds compared
313 with the aluminum based coagulants, whereas the HPI removal by the four coagulants was
314 fairly comparable (<5% difference). Although coagulation with ACH gave a considerably
315 lower removal in HPO compounds compared with the iron based coagulants, it led to a

316 similar reduction in permeate flux decline as FeCl_3 and $\text{Fe}_2(\text{SO}_4)_3$. This might suggest that
 317 the hydrophilic compounds played a more important role in determining the flux performance
 318 for the ceramic membrane, since hydrophobic interaction between the organic compounds
 319 and membrane materials would not be significant due to the highly hydrophilic nature of the
 320 ceramic membrane [5].



321
 322 **Fig.6** AOM fractions before and after coagulation.

323

324 3.7 Membrane fouling analysis

325 In order to investigate the influence of coagulation on the fouling of the ceramic MF
 326 membrane in the filtration of the AOM solutions, the classic filtration models were fit by the
 327 experimental flux data. The R^2 values obtained by fitting the flux data were used to indicate
 328 the major fouling mechanism for the AOM feed solutions with and without coagulation pre-
 329 treatment (Table 2).

330

331 The best fit (with the highest R^2 value) of the experimental data for the non-coagulated AOM
 332 solution was the cake filtration model. This was consistent with our previous study that the
 333 majority of flux decline during the MF of AOM with the ceramic membrane was attributed to
 334 the formation of a cake layer on the membrane surface [7]. The highest R^2 values for the
 335 coagulated AOM feed solutions were given by the intermediate blocking model, except for

336 the alum-treated solution. The shift of filtration mode before and after coagulation was most
 337 likely attributed to the removal of large MW biopolymer molecules during the coagulation
 338 process. Therefore, the improved flux resulting from the coagulation with ACH, $\text{Fe}_2(\text{SO}_4)_3$
 339 and FeCl_3 would be due to the mitigation of the formation of a cake layer by the high MW
 340 molecules [7].

341

342 The best fit for the alum-treated AOM feed solution was cake filtration. One possible
 343 explanation is that the alum-treated AOM solution contained a greater amount of HPO
 344 compounds (as shown in Fig.6) compared with the solutions treated with the other
 345 coagulants. These HPO compounds may aggregate together on the membrane surface via
 346 hydrophobic interaction during the MF process. This mechanism is supported by our
 347 previous findings that the HPO compounds played a very important role in cake layer
 348 formation on the membrane surface [7]. However, due to the high MW compounds being
 349 largely removed from the AOM solution during the coagulation process, the cake layer would
 350 be lower in thickness compared with the un-treated AOM solution, resulting in the
 351 substantially improved flux.

352

353 **Table 2** Summary of the R^2 values for the AOM solutions with and without coagulation pre-
 354 treatment.

Model	Non- coagulated	ACH	Alum	Ferric sulphate	Ferric chloride
Complete blocking	0.9195	0.8808	0.8626	0.6296	0.7931
Intermediate blocking	0.9559	0.9268	0.9003	0.8932	0.9437
Standard blocking	0.9869	0.6654	0.7488	0.6332	0.7154
Cake filtration	0.9884	0.9107	0.9176	0.6705	0.9007

355

356 **4 Conclusions**

357 The effect of the four commonly used water treatment coagulants (i.e., alum, ACH,
358 ferric sulphate and ferric chloride) on mitigation of the fouling of a ceramic MF membrane
359 caused by the AOM released from *Microcystis aeruginosa* was investigated. Treatment of
360 the AOM solutions with the four coagulants led to marked reductions in both the reversible
361 and irreversible fouling for the ceramic MF membrane at the optimal coagulant dosages.
362 ACH, ferric chloride and ferric sulphate performed similarly in reducing the flux decline, while
363 alum gave a considerably lower reduction in flux decline. Organic matter characterization
364 using LC-OCD, fluorescence EEMs as well as carbohydrate and protein quantification
365 indicated that the enhanced membrane performance was primarily due to the effective
366 removal of the very high MW biopolymers ($\gg 20,000$ Da) and hence the mitigation of the
367 formation of the thick cake layer on the membrane surface. Although the cost of ACH, ferric
368 chloride and ferric sulphate was fairly comparable (i.e. \$ 0.03, \$ 0.02 and 0.04 kL⁻¹,
369 respectively), the iron-based coagulants caused a drastic drop in pH for the feed water,
370 which would lead to a considerable increase in the treatment cost due to the necessary pH
371 adjustment. As such, ACH appeared to be a more cost-effective coagulant in maintaining the
372 performance of the ceramic MF membrane systems during cyanobacterial bloom events. It
373 is suggested that further investigations should be conducted in order to gain a better insight
374 into the key mechanism controlling the removal of the high MW biopolymer molecules, with a
375 view to further optimizing the coagulation process.

376

377

378 **References**

379 [1] B. Hofs, J. Ogier, D. Vries, E.F. Beerendonk, E.R. Cornelissen, Comparison of ceramic
380 and polymeric membrane permeability and fouling using surface water, Separation and
381 Purification Technology, 79 (2011) 365-374.

382 [2] L. Dramas, J.P. Croué, Ceramic membrane as a pretreatment for reverse osmosis:
383 Interaction between marine organic matter and metal oxides, *Desalination and Water*
384 *Treatment*, 51 (2013) 1781-1789.

385 [3] S.G. Lehman, L. Liu, Application of ceramic membranes with pre-ozonation for treatment
386 of secondary wastewater effluent, *Water Research*, 43 (2009) 2020-2028.

387 [4] J. Fang, X. Yang, J. Ma, C. Shang, Q. Zhao, Characterization of algal organic matter and
388 formation of DBPs from chlor(am)ination, *Water Research*, 44 (2010) 5897-5906.

389 [5] E.S. Reichwaldt, A. Ghadouani, Effects of rainfall patterns on toxic cyanobacterial blooms
390 in a changing climate: Between simplistic scenarios and complex dynamics, *Water*
391 *Research*, 46 (2012) 1372-1393.

392 [6] N. Her, G. Amy, H.-R. Park, M. Song, Characterizing algogenic organic matter (AOM)
393 and evaluating associated NF membrane fouling, *Water Research*, 38 (2004) 1427-1438.

394 [7] X. Zhang, L. Fan, F.A. Roddick, Understanding the fouling of a ceramic microfiltration
395 membrane caused by algal organic matter released from *Microcystis aeruginosa*, *Journal of*
396 *Membrane Science*, 447 (2013) 362-368.

397 [8] H.K. Shon, S. Vigneswaran, S.A. Snyder, Effluent organic matter (EfOM) in wastewater:
398 Constituents, effects, and treatment, *Crit. Rev. Environ. Sci. Technol.*, 36 (2006) 327-374.

399 [9] L. Fan, T. Nguyen, F.A. Roddick, J.L. Harris, Low-pressure membrane filtration of
400 secondary effluent in water reuse: Pre-treatment for fouling reduction, *Journal of Membrane*
401 *Science*, 320 (2008) 135-142.

402 [10] Z. Liang, Y. Wang, Y. Zhou, H. Liu, Coagulation removal of melanoidins from
403 biologically treated molasses wastewater using ferric chloride, *Chemical Engineering*
404 *Journal*, 152 (2009) 88-94.

405 [11] M. Kabsch-Korbutowicz, Effect of Al coagulant type on natural organic matter removal
406 efficiency in coagulation/ultrafiltration process, *Desalination*, 185 (2005) 327-333.

407 [12] Y. Goh, J. Harris, F. Roddick, Impact of *Microcystis aeruginosa* on membrane fouling in
408 a biologically treated effluent, *Water science and technology*, 63 (2011) 2853-2859.

409 [13] R. Resson, F.S. Soong, J. Fitzgerald, L. Turczynowicz, O.E. Saadi, D. Roder, T.
410 Maynard, I. Falconer, Health Effects Of Toxic Cyanobacteria (Blue-Green Algae), in,
411 National Health and Medical Research Council of Australia, 1994.

412 [14] C.J.S. Bolch, S.I. Blackburn, Isolation and purification of Australian isolates of the toxic
413 cyanobacterium *Microcystis aeruginosa* Kütz, *Journal of Applied Phycology*, 8 (1996) 5-13.

414 [15] N. Gao, M. Li, W. Jing, Y. Fan, N. Xu, Improving the filtration performance of ZrO_2
415 membrane in non-polar organic solvents by surface hydrophobic modification, *Journal of*
416 *Membrane Science*, 375 (2011) 276-283.

417 [16] M. Dubois, K.A. Gilles, J.K. Hamilton, P.A. Rebers, F. Smith, Colorimetric method for
418 determination of sugars and related substances, *Analytical Chemistry*, 28 (1956) 350-356.

419 [17] M. Bahram, R. Bro, C. Stedmon, A. Afkhami, Handling of Rayleigh and Raman scatter
420 for PARAFAC modeling of fluorescence data using interpolation, *Journal of Chemometrics*,
421 20 (2006) 99-105.

422 [18] S.A. Huber, A. Balz, M. Abert, W. Pronk, Characterisation of aquatic humic and non-
423 humic matter with size-exclusion chromatography - organic carbon detection - organic
424 nitrogen detection (LC-OCD-OND), *Water Research*, 45 (2011) 879-885.

425 [19] G.R. Aiken, D.M. McKnight, K.A. Thorn, E.M. Thurman, Isolation of hydrophilic organic
426 acids from water using nonionic macroporous resins, *Organic Geochemistry*, 18 (1992) 567-
427 573.

428 [20] J. Herima, Constant pressure blocking filtration laws. Application to power-law non-
429 Newtonian fluids, *Trans. Ind. Chem. Eng*, 60 (1982) 183.

430 [21] Y. Shen, W. Zhao, K. Xiao, X. Huang, A systematic insight into fouling propensity of
431 soluble microbial products in membrane bioreactors based on hydrophobic interaction and
432 size exclusion, *Journal of Membrane Science*, 346 (2010) 187-193.

433 [22] F. Qu, H. Liang, J. Zhou, J. Nan, S. Shao, J. Zhang, G. Li, Ultrafiltration membrane
434 fouling caused by extracellular organic matter (EOM) from *Microcystis aeruginosa*: Effects of
435 membrane pore size and surface hydrophobicity, *Journal of Membrane Science*, 449 (2014)
436 58-66.

437 [23] R.K. Henderson, A. Baker, S.A. Parsons, B. Jefferson, Characterisation of algogenic
438 organic matter extracted from cyanobacteria, green algae and diatoms, *Water Research*, 42
439 (2008) 3435-3445.

440 [24] W. Chen, P. Westerhoff, J.A. Leenheer, K. Booksh, Fluorescence Excitation-Emission
441 Matrix Regional Integration to Quantify Spectra for Dissolved Organic Matter, *Environmental
442 Science and Technology*, 37 (2003) 5701-5710.

443 [25] X. Zhang, L. Fan, F.A. Roddick, Influence of the characteristics of soluble algal organic
444 matter released from *Microcystis aeruginosa* on the fouling of a ceramic microfiltration
445 membrane, *Journal of Membrane Science*, 425–426 (2013) 23-29.

446 [26] J. Haberkamp, A.S. Ruhl, M. Ernst, M. Jekel, Impact of coagulation and adsorption on
447 DOC fractions of secondary effluent and resulting fouling behaviour in ultrafiltration, *Water
448 Research*, 41 (2007) 3794-3802.

449 [27] J.P.L. Kenney, J.B. Fein, Importance of extracellular polysaccharides on proton and Cd
450 binding to bacterial biomass: A comparative study, *Chemical Geology*, 286 (2011) 109-117.

451 [28] S. Meng, M. Rzechowicz, H. Winters, A.G. Fane, Y. Liu, Transparent exopolymer
452 particles (TEP) and their potential effect on membrane biofouling, *Applied microbiology and
453 biotechnology*, 97 (2013) 5705-5710.

454 [29] A.M. McIntyre, C. Guéguen, Binding interactions of algal-derived dissolved organic
455 matter with metal ions, *Chemosphere*, 90 (2013) 620-626.

456 [30] J.-D. Lee, S.-H. Lee, M.-H. Jo, P.-K. Park, C.-H. Lee, J.-W. Kwak, Effect of coagulation
457 conditions on membrane filtration characteristics in coagulation-microfiltration process for
458 water treatment, *Environmental Science & Technology*, 34 (2000) 3780-3788.

459 [31] L. Fan, T. Nguyen, F.A. Roddick, Characterisation of the impact of coagulation and
460 anaerobic bio-treatment on the removal of chromophores from molasses wastewater, *Water
461 Research*, 45 (2011) 3933-3940.

462 [32] T. Takaara, D. Sano, H. Konno, T. Omura, Affinity isolation of algal organic matters able
463 to form complex with aluminium coagulant, *Water Science and Technology*, 4 (2004) 95-102.
464